ACS APPLIED MATERIALS & INTERFACES

Research Article

www.acsami.org

Creating Antibacterial Surfaces with the Peptide Chrysophsin-1

Ivan E. Ivanov,[†] Alec E. Morrison,[‡] Jesse E. Cobb,[†] Catherine A. Fahey,[†] and Terri A. Camesano*,[†]

[†]Department of Chemical Engineering, and [‡]Department of Chemistry and Biochemistry, Worcester Polytechnic Institute, Worcester, Massachusetts 01609, United States

Supporting Information

ABSTRACT: Immobilization of antimicrobial peptides (AMPs) holds potential for creating surfaces with bactericidal properties. In order to successfully incorporate AMPs into desired materials, increased fundamental understanding of the relationship between AMP immobilization and the efficacy of bound peptides as antibacterial agents is required. In this study, we characterize the relationship between surface binding of the AMP and subsequent ability of the peptide to kill bacteria. Surface immobilization of the AMP chrysophsin-1 (CHY1) via a flexible linker is studied in real-time, using a quartz crystal microbalance with dissipation monitoring (QCM-D). Depending on whether the AMP is physically adsorbed to the surface or attached covalently via a zero-length or flexible cross-linker, changes could be observed in AMP orientation, surface density, flexibility, and activity against bacteria. Covalent surface binding of CHY1 led to the formation of solvated monolayers of vertically positioned peptide molecules, while the physical adsorption of CHY1 led to the deposition of rigid monolayers of horizontally positioned peptide molecules on the sensor surface. Covalently bound peptides were not removed by extensive washing and did not leach from the surface. Zero-length immobilization of the peptide decreased its ability to kill *E. coli* to 34% ± 7% of added bacteria, while binding via a flexible linker resulted in 82% ± 11% of bacteria being killed by the AMP.

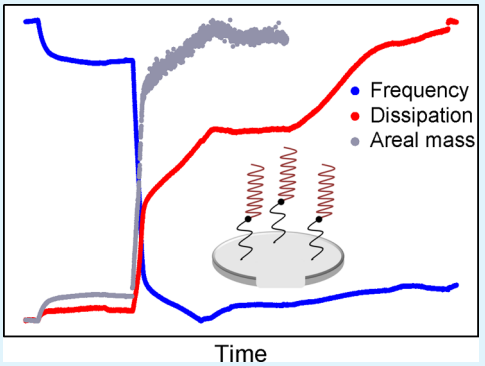

KEYWORDS: *antimicrobial peptides, immobilization, QCM-D, flexible cross-linker, bactericidal activity, real-time monitoring*

INTRODUCTION

Pathogenic bacteria such as *Escherichia coli*, *Listeria monocytogenes*, and *Salmonella spp.* have been shown to cause 9.4 million illnesses per year, leading to almost 56 000 hospitalizations and over 1300 deaths.[1−3] Contaminations occur predominantly during the food processing steps, and studies have demonstrated that even the proper use of sanitization techniques can leave viable micro-organisms on the working surfaces.[4] In order to prevent the development of foodborne illnesses, as well as to reduce the rates of hospital-acquired and biomaterial-associated infections, researchers have attempted to engineer surfaces with antimicrobial properties. These can be generally classified into three broad categories: microbe-repelling, contact-active, and biocide-releasing surfaces.[5] The majority of contact-active techniques utilize polymeric substances (e.g., poly(4-vinylpridine)[6] and poly(ethyleneimine)[7]), quaternary ammonium compounds[8,9] or metallic compounds[10] to render antimicrobial properties to surfaces. These methods rely on the disruption of the bacterial cell wall[11] or on the removal of structurally critical membrane ions.[12] More recently, the use of antimicrobial peptides for the development of contact-killing surfaces has also been investigated.[13]

Antimicrobial peptides (AMPs) are naturally occurring substances that are able to kill bacteria and fungi, usually through cell lysis.[14] AMPs often exhibit high structural stability and ability to refold after exposure to heat and desiccation.[15,16] Cationic AMPs, usually 10−50 amino acids in length and possessing amphipathic structure with charges ranging from +2 to +9, represent an important class of macromolecules because of their activity against microbes. Their charge and hydrophobicity are considered the underlying features that enable binding and subsequent antimicrobial activity.[17−19] These AMPs create pores in the cell membrane, disrupting the osmotic balance and leading to cell lysis, even though the exact mechanism is still under investigation.[20−22] The most widely recognized mechanisms are the barrel-stave, toroidal, and carpet models.[23] In the barrel-stave and toroidal theories, peptide molecules insert themselves in the lipid membrane forming a bundle with a cylindrical central lumen, or causing continuous bending of the lipid monolayer in a toroidal pore, respectively, which results in the loss of cellular constituents. The carpet mechanism proposes that peptides coat the outer membrane surface and induce membrane disintegration by formation of micelles.[24]

Surface immobilization of antimicrobial peptides thus represents an attractive contact-killing technique due to the AMP's stability, broad range of action, and the low likelihood for development of microbial resistance.[13] Tethering of AMPs can further reduce leaching, proteolysis, and cytotoxicity associated with certain peptides.[25,26] Various approaches for AMP immobilization have been reported in the literature including a wide variety of substrates (contact lenses,[27]

Received: August 2, 2012
Accepted: October 8, 2012
Published: October 8, 2012

   dx.doi.org/10.1021/am301530a | ACS Appl. Mater. Interfaces 2012, 4, 5891−5897

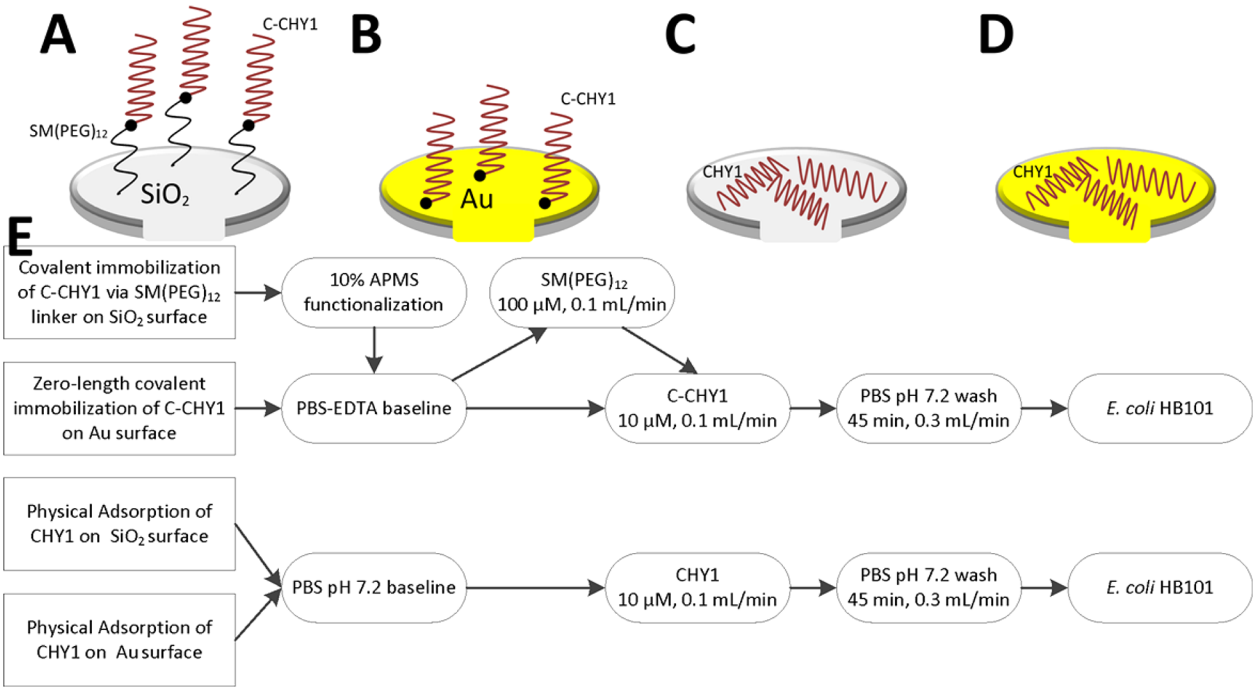

Figure 1. Diagram of the peptide immobilization mechanisms (not drawn to scale) and schematic representation of the immobilization procedure. (A) Cysteine modified chrysophsin-1 (C-CHY1) was immobilized via a flexible PEG spacer, $SM(PEG)_{12}$, to amine-coated silicon dioxide QCM-D crystals. (B) C-CHY1 was immobilized via zero-length covalent binding of its cysteine group to the gold surface of QCM-D sensors. (C) Chrysophsin-1 was physically adsorbed to the surface of silicon dioxide QCM-D crystals. (D) CHY1 was physically adsorbed to the surface of gold QCM-D crystals. (E) Immobilization reactions were conducted in parallel, with the exception of mechanism-specific steps, in order to minimize environmental interference to the QCM-D frequency and dissipation signals.

polyamide resins,[28] polymer brushes[29,30] and resins,[31−33] glass,[34] titanium[35]) and choice of immobilization chemistry involved, such as formation of amide bonds,[27,36] disulfide bridges,[37] the use of thiol groups for binding to maleimide- or epoxide-modified surfaces,[35,38] and Huisgen 1,3-dipolar cycloaddition.[39] Most protocols also utilize a flexible spacer, commonly polyethylene glycol (PEG), between the surface and the peptide to allow for the AMP's laterally unrestricted movement and bacterial membrane penetration.[31−33,35,36] Results overall indicate that AMPs can be successfully immobilized on surfaces, however, with suboptimal antimicrobial efficiency.[31−33] Furthermore, the importance of polymeric spacers is still controversial as studies often indicate that AMPs lose their bactericidal properties upon zero-length surface immobilization,[35,40] while some report that spacers of only two to six C atoms may allow peptides to efficiently kill bacteria.[28] This has led to the development of alternative hypotheses for the AMP's mode of action, such as by disturbing the ionic balance on the membrane surface.[41] In addition, little is known about the orientation of the tethered peptide and its importance in the membrane permeation process. As a result, Onaizi and Leong highlight the need for real-time monitoring of peptide immobilization in order to better understand and optimize the process.[25]

The QCM-D has emerged as a convenient technique to monitor events at a surface nondestructively in real-time. This technique has been applied to a variety of applications ranging from the study of proteins, lipid vesicles or cells, to monitoring gas absorption in polymeric films and corrosion of fuel cell electrodes.[42−44] According to the conventional mass-loading theory, deposition of a substance to the surface of the QCM-D sensor will lead to a decrease in its resonating frequency and may lead to energy dissipation. The amount of energy lost will depend on the rigidity of the film, where soft layers are more prone to dissipative losses than rigid layers.[45]

The aim of this study was to characterize how the fundamental activity of the AMP chrysophsin-1 is affected by surface immobilization. Physical adsorption of the AMP and covalent surface binding with or without a flexible spacer was monitored using QCM-D in real-time. The immobilization method used to attach chrysophsin-1 to the surface affected the AMP orientation, surface density, flexibility, and activity against bacteria. The immobilized peptide orientation on the surface was correlated to its bactericidal activity and a mode of action was proposed, leading to new insight into the mechanism by which bound AMPs inactivate bacteria.

MATERIALS AND METHODS

Bacterial Culture and Harvesting. *Escherichia coli* HB101 (ATCC 33694) was cultured overnight in 50 mL of Luria−Bertani (LB) broth. For toxicity studies, the optical density of overnight cultures was adjusted to OD_{600} = 1.0 and cells were washed once in with 0.01 M phosphate buffered saline adjusted to pH 7.2 (PBS pH 7.2) for 1 min at 13 200 rpm. For QCM-D experiments, *E. coli* were washed once with PBS (pH 7.2) by centrifugation for 10 min at 10 000 rpm and diluted 100-fold.

Peptides. Chrysophsin-1[46] (CHY1; FFGWLIKGAIHAGKAIHGLIHRRRH) and CHY1 modified with a N-terminal cysteine residue (C-CHY1; CFFGWLIKGAIHAGKAIHGLIHRRRH) were purchased from Bachem Americas, Inc. (Torrance, CA). Peptide structure and purity (95% or greater) were confirmed with matrix-assisted laser desorption/ionization mass spectroscopy and high-performance liquid chromatography, respectively. Lyophilized CHY1 and C−CHY1 were

resuspended in PBS (pH 7.2) and PBS (pH 7.2) supplemented with 1 mM ethylenediaminetetraacetic acid (PBS-EDTA), respectively, to a concentration of 5 g/L, and stored at −20 °C.

Toxicity Studies. The bactericidal activity of CHY1 and C-CHY1 was tested against *E. coli*. After harvesting, 5 aliquots of bacterial culture were diluted to a concentration of ∼2 × 10^5 colony-forming units/mL (CFU/mL). Peptides were added to four bacterial dilutions to yield a final concentration of 10 μM and the fifth dilution was used as a negative control. After a 1 hour incubation at room temperature, 0.1 mL aliquots of each suspension were spread on LB agar and incubated overnight. The number of CFUs was counted and the toxicity of each peptide was quantified as the percentage decrease in CFUs compared to control samples. Experiments were performed in triplicate.

QCM-D: Peptide Covalent Linking. Silicon dioxide and gold crystals (Biolin Scientific, Sweden) were used for chemical immobilization experiments of C-CHY1. The SiO_2 crystals were cleaned at 40 °C with 2% sodium dodecyl sulfate (SDS) followed by 45 s etching in an oxygen plasma cleaner (SPI Supplies, PA). The Au crystals were cleaned with basic piranha solution (5:1:1 water, hydrogen peroxide, 30% ammonia hydroxide) followed by 45 s of oxygen plasma treatment. The cleaned SiO_2 crystals were submerged in 10% (3-aminopropyl)trimethoxysilane in methanol for 20 min before being placed in the QCM-D chambers. A Q-Sense E4 system (Biolin Scientific, Sweden) was used for monitoring the frequency and dissipation changes in the 3rd through 11th overtones during peptide surface immobilization. Measurements were taken at a constant temperature of 23 °C, and solutions were flowed at a rate of 0.1 mL/min, unless otherwise specified. Buffers for QCM-D experiments were degassed by sonication under negative pressure for 30 min. Amounts of solutions used for QCM-D experiments are listed on a per-chamber basis. After crystal cleaning and functionalization, PBS-EDTA buffer was used to establish a stable baseline. Next, 1 mL of 100 μM succinimidyl-[(*N*-maleimidopropionamido)-dodecaethyleneglycol] ester ($SM(PEG)_{12}$, Thermo Fisher Scientific, Inc., IL) cross-linker was flowed over the SiO_2 crystals and allowed to incubate for 30 min. Both Au and SiO_2 crystals were then rinsed with 1 mL of PBS-EDTA buffer before 1 mL of 10 μM C-CHY1 samples were introduced and incubated for an additional 30 min. After the incubation, PBS (pH 7.2) was flowed over the crystals for 45 min at 0.3 mL/min to remove any unbound peptide. Once rinsed, 2.5 mL of diluted bacterial culture was flowed and left to incubate for 1 h. Following the incubation period, the crystals were rinsed with 2 mL of PBS (pH 7.2) buffer before being removed and placed in 0.85% saline solution for staining. Covalent linking experiments were repeated three times in two parallel chambers. A schematic representation of the immobilization procedure is presented in Figure 1.

QCM-D: Peptide Physical Adsorption. Gold and silicon dioxide crystals were used for physical adsorption experiments of CHY1. Crystals were cleaned as described in the previous section. The crystals were placed in the QCM-D chambers and PBS buffer (pH 7.2) was pumped to establish a stable baseline. Following baseline establishment, 1 mL of 10 μM CHY1 samples were flowed through each chamber and incubated for 30 min. The crystals where then rinsed with PBS buffer (pH 7.2) for 45 min at 0.3 mL/min. After the rinse, 2.5 mL of diluted bacterial culture was flowed and allowed to incubate for 1 h. The crystals were then rinsed with 2 mL of PBS buffer (pH 7.2) before being removed and placed in 0.85% saline solution for staining. Physical adsorption experiments were repeated three times in two parallel chambers.

QCM-D: Data Modeling. QCM-D data from the third overtone was used for data modeling. Areal mass density of molecules on the sensor surface was determined using the Sauerbrey equation[47] for films with $\Delta D < 1 \times 10^{-6}$ or using the extended Voigt−Kelvin model[48] otherwise. Bulk fluid density and viscosity were taken as, respectively, 1000 kg/m^3 and 0.001 kg/m×s. Film density of 1000 kg/m^3 was also assumed.[49] A unique fit of the extended Voigt−Kelvin model was obtained in all cases.

The $\Delta D/\Delta f$ ratio, indicative of the intrinsic viscosity of film components in acoustic sensors,[50] was also determined for the immobilized peptides based on the frequency and dissipation data from the third overtone at the end of the peptide incubation period.

Bacterial Viability. Bacterial viability was characterized following QCM-D experiments. The crystals were stained in 5 μM SYTO 9 and 30 μM propidium iodide using a LIVE/DEAD *Bac*Light Bacterial Viability Kit (Life Technologies Corp, NY) in 0.85% saline solution for 15 min. The stained crystals were rinsed once with saline solution to remove excess dye and images of bacteria were examined with a 20× objective using FITC and Texas Red filters under a Nikon Eclipse E400 fluorescence microscope. Captured images were merged using the software SPOT Advanced and the percentage of viable cells was determined. At least five different locations were analyzed per crystal.

Peptide Leaching. In order to test peptide leaching after the immobilization process, QCM-D crystals from each set of experiments (Figure 1) were removed from the instrument after the 45-min buffer wash and incubated in 2 mL of PBS (pH 7.2) under 70 rpm rotation. The supernatants were collected and mixed with harvested *E. coli* HB101 cells to a final concentration of ∼5 × 10^4 CFU/mL. The samples were incubated for 1 h at room temperature and 50-μL aliquots of 10-fold dilutions were plated on LB agar. After overnight incubation, the number of CFUs was counted and compared to a negative control of cell incubated in PBS (pH 7.2).

RESULTS

Peptide Toxicity. The bactericidal activities of 10 μM CHY1 and C−CHY1 were tested against *E. coli* in order to confirm that the cysteine modification did not compromise the activity of the AMP. Both peptides demonstrated >99.9% killing with no statistically significant difference between the results. This indicated that CHY1 and C-CHY1 exhibit equivalent bactericidal activity at the tested concentration.

Covalent Surface Immobilization. The surface immobilization of chrysophsin-1 via a flexible PEG spacer and using zero-length covalent binding was monitored in real-time using QCM-D. Figure 2 shows frequency change, Δf, and energy dissipation response, ΔD, in the 3rd through 11th overtones for zero-length immobilization of C-CHY1 on a gold surface. The adsorption of peptide decreased Δf by ∼220 Hz and increased ΔD by ∼36 × 10^{-6} for the 3rd overtone (all frequency and dissipation values reported in this text correspond to data from the 3rd overtone, unless stated otherwise). This change in frequency and dissipation occurred in two steps (at 7 and 48 min) as peptide remaining in the instrument tubing also bound to the sensor after the incubation period was ended, suggesting

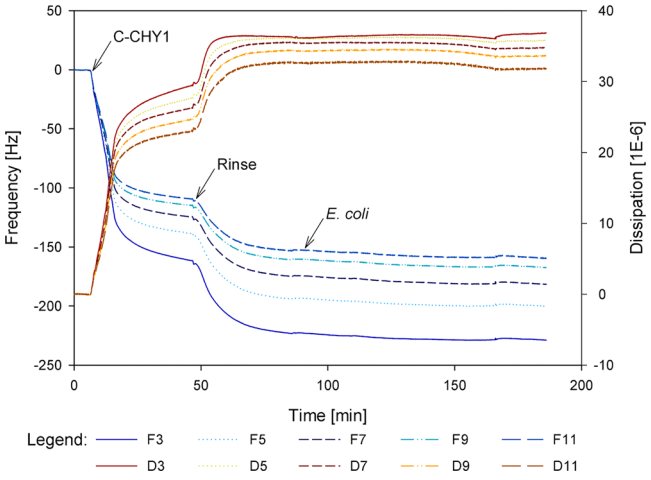

Figure 2. Frequency and dissipation response from the 3rd through 11th overtones for the zero-length covalent immobilization of C-CHY1 onto gold surface. Binding of C-CHY1 resulted in 220 Hz decrease in frequency and 36×10^{-6} increase in energy dissipation for the 3rd overtone. The immobilized peptide was not removed by extensive rinsing.

that the surface was initially not saturated. The buffer rinse caused no peptide detachment.

Figure 3 shows the real-time frequency and dissipation monitoring of C-CHY1 covalent immobilization on a silicon

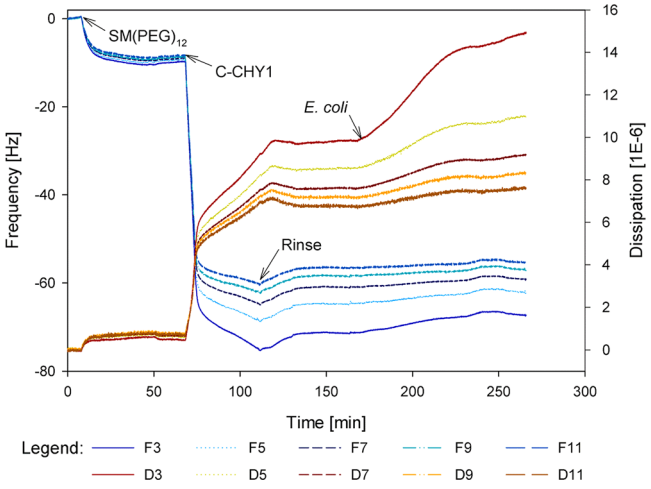

Figure 3. Frequency and dissipation response from the 3rd through 11th overtones for the covalent immobilization of C-CHY1 on a silicon dioxide surface using a flexible PEG spacer. The $SM(PEG)_{12}$ linker was attached at 137 ng/cm^2, as indicated by a fit to the Sauerbrey equation. Binding of the peptide to the linker resulted in frequency decrease of 60 Hz and increase in dissipation of 9×10^{-6}. A buffer rinse removed only unbound peptide molecules.

dioxide surface via a flexible linker. Binding of the $SM(PEG)_{12}$ cross-linker to the amine-functionalized sensor caused a 10 Hz decrease in frequency and a $<1 \times 10^{-6}$ increase in dissipation. Rinsing after the incubation period led to little or no removal of unbound $SM(PEG)_{12}$ molecules. Upon its addition to the crystals, C-CHY1 rapidly attached to the surface via the linker as indicated by the immediate drop in Δf of ~60 Hz and increase in ΔD of 9×10^{-6}. Rinsing off the weakly bound C-CHY1 molecules caused a small (<5%) frequency and dissipation change, indicating that the immobilized peptide was not removed from the surface. The introduction of *E. coli* HB101 cells resulted in Δf and ΔD shifts over the 11 overtones, which may allow for the determination of the bond stiffness between the surface and the cell body (see the Supporting Information).

Physical Adsorption. The physical adsorption of CHY1 onto silicon dioxide and gold surfaces was also tested. Adsorption of CHY1 on a gold QCM-D sensor decreased Δf by ~9 Hz, while ΔD remained virtually unchanged at zero, indicating that the peptide adsorbed as a rigid laterally homogeneous film (Figure 4). The buffer wash increased the frequency by 4 Hz, suggesting that peptide is detaching from the crystal as a result of the shear stress caused by the flow.

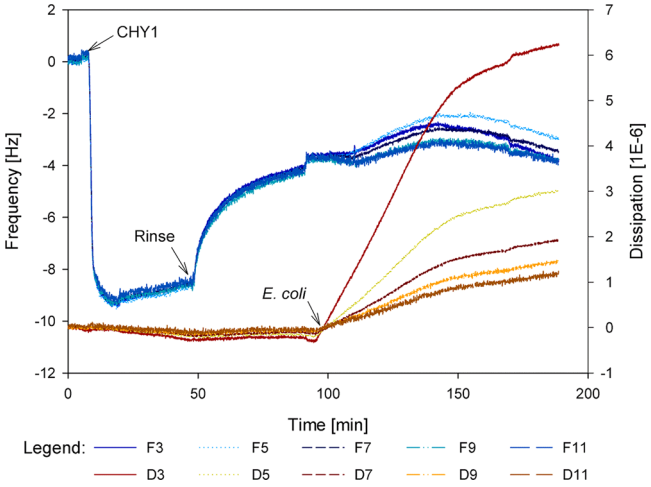

Figure 4. Frequency and dissipation response from the 3rd through 11th overtones for the physical adsorption of CHY1 on a gold surface. The peptide adsorbed as a monolayer at 72.7 ng/cm^2, as indicated by a fit to the Sauerbrey equation, and was partially removed by the buffer rinse.

The introduction of CHY1 led to rapid physical adsorption onto the bare silicon dioxide surface, as indicated by the drop in Δf of ~9 Hz (Figure 5). The decrease in frequency was

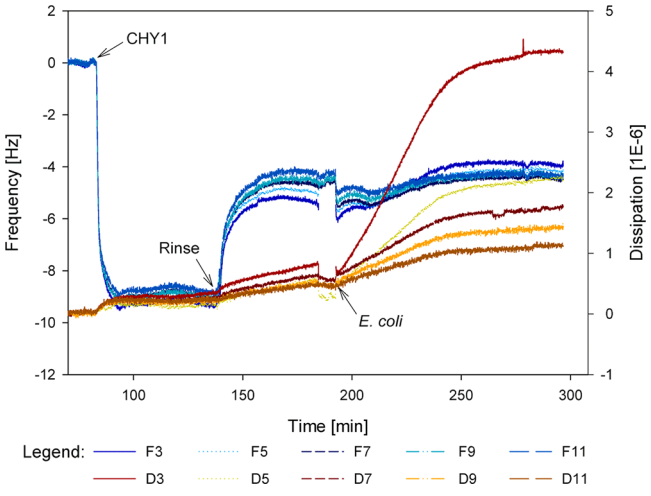

Figure 5. Frequency and dissipation response from the 3rd through 11th overtones for physical adsorption of CHY1 on a silicon dioxide surface. The peptide adsorbed as a monolayer at 93.5 ng/cm^2 and was partially removed by the buffer rinse.

accompanied by an increase in dissipation of roughly 0.3×10^{-6}, which suggests that CHY1 was also adsorbed as a rigid layer onto the silicon dioxide surface. Rinsing the weakly adsorbed peptide caused an increase in Δf of ~4 Hz, while ΔD increased slightly, still remaining below 1×10^{-6}.

Immobilized Peptide Density and Intrinsic Viscosity. The Sauerbrey equation and the Voigt–Kelvin viscoelastic model were used to determine the amount of peptide immobilized onto the QCM-D sensors. Chrysophsin-1 adsorbed in similar amounts on the silicon dioxide and gold surfaces at, respectively, 93.5 and 72.7 ng/cm^2 after rinsing (Table 1). Calculations assuming length and width of the CHY1 α-helix of 3.5 and 1.2 nm, respectively, indicate that the peptide adsorbs as a monolayer on the sensor surfaces. Covalent binding of C–CHY1 onto the gold sensor immobilized 4610 ng/cm^2 of peptide, while linking of C-CHY1 through SM(PEG)$_{12}$ on the silicon dioxide surface resulted in 2080 ng/cm^2 of bound substance (binding of the SM(PEG)12 linker contributed 138 ng/cm^2). Since the QCM-D is sensitive to the mass of solvent trapped in solvated films,[49] the areal mass density reported for C-CHY1 chemically linked to gold and silicon dioxide surfaces includes the masses of both the peptide and the trapped buffer.

Table 1. Peptide Immobilization Parameters and Bactericidal Activity against *E. coli* HB101

immobilization method	areal mass[a] [ng/cm^2]	$(\Delta D_3)/(-\Delta f_3/3)$[b] [$\times 10^{-6}$/Hz]	bacterial killing [%]
	Silicon Dioxide Surface		
physical adsorption	93.5	0.03 ± 0.01	19 ± 1
covalent linking	138 (linker)	0.05 ± 0.01 (linker)	82 ± 11
	2080 (peptide)	0.13 ± 0.03 (peptide)	
	Gold Surface		
physical adsorption	72.7	0.03 ± 0.01	53 ± 16
covalent linking	4610	0.15 ± 0.02	34 ± 7

[a]Calculated after buffer rinse based on frequency and dissipation data from the 3rd overtone. [b]Calculated before buffer rinse based on frequency and dissipation data from the 3rd overtone.

The $\Delta D/\Delta f$ ratio for the third overtone was also determined in order to obtain information about the intrinsic viscosity of the film components.[51] The physically adsorbed peptides and the SM(PEG)$_{12}$ linker registered very small $\Delta D/\Delta f$ values, suggesting that these films behave rather elastically. Covalent linking of C-CHY1 resulted in much more viscous films with $\Delta D/\Delta f$ values of 0.13 ± 0.03 and 0.15 ± 0.02 when immobilized on silicon dioxide and gold surfaces, respectively.

Immobilized Peptide Activity. Immobilization of C-CHY1 through zero-length cross-linking to a gold surface resulted in 34% ± 7% killing of *E. coli* HB101, while AMP immobilization on a silicon dioxide surface through a flexible PEG spacer killed over 80% of bacterial cells (Table 1). Physical adsorption of the peptide on gold and silicon dioxide surfaces led to 53% ± 16% and 18.7% ± 1.4% bacterial killing, respectively. A statistically significant difference ($P < 0.05$) in the peptide bactericidal activity was found between all four immobilization techniques, based on the Kruskal–Wallis One Way ANOVA on Ranks test.

Immobilized Peptide Release. Peptide leaching from the surface was not observed in quantities sufficient to kill bacterial cells. No statistically significant difference ($P = 0.609$, One Way ANOVA on Ranks) in the number of CFUs was observed for *E. coli* incubated with supernatants from QCM-D crystals with immobilized peptides vs *E. coli* incubated in the PBS buffer (pH 7.2) (data not shown).

DISCUSSION

Immobilization of antimicrobial peptides can be used to create contact-killing surfaces with a wide range of applications. Although the activity of AMPs in solution has been well-documented, the mechanisms of actions of AMPs against *E. coli* and other bacteria are still not fully understood. Furthermore, even less is known about how surface-bound AMPs are able to inactivate bacteria, in comparison to AMPs in solution. Generally, it is agreed that surface tethering of AMPs with no spacer or using very short spacer molecules leads to a reduction in the peptide's toxicity toward bacterial cells.[27,32,35] However, some groups report good bactericidal activity of AMPs directly bound to the surface,[41] albeit at a much higher peptide concentration.[28] Studies employing spacer molecules, usually PEG derivatives with molecular weights ranging from 3000 Da to 5400 Da, often demonstrate high bactericidal activity of the bound AMP.[29,33,35,36] Still, Bagheri et al. have reported that, in certain cases, PEG spacers of molecular weight as high as 3000 Da could lead to reduction in antimicrobial activity of several orders of magnitude.[31] An additional concern regarding AMP immobilization methodologies is that peptide leaching from the surface has been observed[33] and, often, is not tested.[27,29,31,32,35,36]

In this study, we observed a significant decrease in bactericidal activity of C-CHY1 against *E. coli* when immobilized through zero-length covalent linking, while immobilization of C-CHY1 via a flexible PEG-derived linker preserved 82% ± 11% of the killing activity of the AMP (Table 1). Experiments on the peptides' toxicity in liquid culture allow us to attribute the reduction of the peptides' performance to limitations of the immobilization technique employed. At the chosen concentration of 10 μM, both peptides killed virtually all bacteria in solution (>99.9%), and the cysteine modification did not affect the bactericidal properties of CHY1. Furthermore, peptide leaching from the surface was not observed in amounts sufficient to kill bacteria.

Since the three major theories on the AMP's mode of action—the barrel-stave, toroidal, and carpet models—require that the peptide molecules be able to adopt a certain conformation on the cell surface, we expect that restricting the peptide's movement will affect its killing activity. However, an immobilization method which allows free movement of the peptide should not significantly affect its bactericidal properties. Zero-length binding of C-CHY1 on the gold sensor demonstrated a mass increase, accompanied by a large increase in dissipation (Figure 2). The loss of energy indicates the deposition of a soft hydrated film. This suggests that C-CHY1 forms a monolayer of vertically positioned peptides, trapping water molecules between them. This arrangement is also electrostatically most favorable, as the peptide molecules are positively charged and will adopt an alignment that minimizes the electrostatic repulsive forces. However, zero-length immobilization restricts the free movement of the peptide and reduces its bactericidal potency. Binding of the SM(PEG)$_{12}$ cross-linker and, subsequently, of C-CHY1 to the amino-functionalized silicon dioxide sensor surface, was also confirmed by the observed decrease in frequency (Figure 3). While the cross-linker did not cause significant energy losses ($\Delta D \leq 1 \times$

10^{-6}), binding of the peptide led to an increase in dissipation, indicating the formation of a hydrated layer. This, combined with the unrestricted range of motion which the linker provides, suggests that the peptide will be able to adopt a conformation favorable for penetrating the bacterial cell wall. The bacterial viability counts corroborate this theory. The buffer rinse performed after the immobilization steps was designed to simulate physical stress under a shear rate of 7.5 s^{-1} for 45 min. We did not observe any removal of C-CHY1 from the gold surface as a result of the rinse, which is consistent with the high strength of the gold−sulfur bond (∼45 kcal/mol[52]). Performing a buffer rinse after the immobilization of C-CHY1 via a flexible linker removed only loosely attached peptide molecules.

Physical adsorption of CHY1 on gold and silicon dioxide surfaces also led to a decrease in frequency, but the dissipation remained almost constant at zero. This indicates that, when not chemically bound to the surface, the peptide adsorbs as a rigid monolayer of molecules horizontally positioned on the sensor. Such a conformation is most favorable because it maximizes the adhesion area. Furthermore, electrostatic interactions should prevent multilayer formation. After being exposed to the physical stress exerted by the buffer rinse, significant peptide removal was observed, indicating that physical adsorption of antimicrobial peptides is not a viable technique for surface coating. Bacterial viability counts indicated limited killing activity against *E. coli*.

Modeling the QCM-D frequency and dissipation changes using the Sauerbrey equation and the Voigt−Kelvin model suggested that CHY1 adsorbs in similar quantities on both silicon dioxide and gold surfaces. However, the areal mass quantities reported for covalent linking of C-CHY1 include the mass contribution of both the adsorbate (peptide molecules) and the solvent (PBS-EDTA buffer), because the QCM-D is sensitive to solvent trapped in hydrated films. Although it was not done here, some researchers have used ellipsometry in conjunction with QCM-D[53] to measure the amounts of trapped solvent and adsorbate on the sensor surface separately, in order to quantify the amount of peptide covalently bound to the gold and silicon dioxide sensors.

According to the classical solution viscosity theory, the grafting density, size, and shape of molecules tethered to a surface will determine the viscosity of the film. The $\Delta D/\Delta f$ ratio in QCM-D can be used to determine the intrinsic viscosity of the adsorbate, which is correlated to the orientation of the molecules in a concentration-independent manner.[54] In this study, we observed that physically adsorbed peptide molecules, forming a horizontal monolayer on the sensor surface, led to low $\Delta D/\Delta f$ values, while covalently end-tethered peptides, which are able to change their orientations in solution, formed viscous films. This approach has been previously used by the Gizeli group to distinguish between single- and double-stranded DNA molecules tethered to a surface, between double-stranded DNA of same shape but various sizes, and between molecules of same mass and size but various shapes.[50,51]

Recent studies have explored the effect of immobilization techniques on changes in the AMP's mode of action. Gao et al.[55] utilized circular dichroism to measure the alpha-helicity of free and bound peptide as it interacts with lipid vesicles, and Bagheri et al.[56] investigated how free and immobilized peptides with different modes of action penetrate the inner and outer membrane of *E. coli*. Although insufficient data are available for the mode of action of CHY1 in solution, it is interesting to speculate that C-CHY1 immobilized through a flexible surface linker may work through the carpet model, in which peptide molecules will coat the cell surface and induce release of lipid micelles from the membrane. This is based on the observation that exposure to the peptide leads to membrane disruption, as suggested by the fluorescence microscopy images, since the propidium iodide dye only penetrates cells with permeabilized membranes. This finding is interesting because the $SM(PEG)_{12}$ cross-linker (5.3 nm) and the C-CHY1 peptide (∼3.5 nm), when immobilized on a surface, will be too short to span the membrane of *E. coli* cells (∼8 nm inner membrane and 8−15 nm outer membrane thickness). Thus, it would be difficult for the AMP to span the thickness of the cell membrane, which would be required for the barrel-stave or toroidal pore models of AMP action. Although further experimentation will be needed to confirm this theory, the suggestion that the carpet model is the active mechanism by which chrysophsin-1 acts against *E. coli* is supported by a recent study in our laboratory, in which QCM-D overtone analysis was used to monitor the penetration of a closely related AMP, chrysophsin-3, into a phosphatidylcholine supported lipid bilayer. Wang et al. observed uniform positive Δf shifts at all overtones after addition of 10 μM chrysophsin-3, which is indicative of membrane disruption through the formation of peptide-lipid aggregates.[22] Mechler el al. also demonstrated lysis of a 1,2-dimyristoyl-*sn*-glycero-3-phosphocholine supported lipid bilayer upon the introduction of high concentrations of the cationic AMPs maculatin and aurein, as confirmed by QCM-D experiments and atomic force microscopy imaging.[57]

CONCLUSIONS

The flexibility and orientation of surface immobilized antimicrobial peptides is thus of great importance for their bactericidal activity and certain immobilization techniques can significantly limit the peptide's ability to adopt a conformation favorable for the penetration of bacterial cell walls. Acoustic sensing techniques represent convenient tools for the real-time monitoring of peptide orientation during the immobilization process and can provide quantitative information about the peptide grafting density or be integrated with other techniques to also obtain *in situ* data about the bactericidal activity of the tethered AMP. Such fundamental information can be used to further elucidate the mechanisms by which bound antimicrobial peptides deactivate microbial cells.

ASSOCIATED CONTENT

Supporting Information

Analysis of the interaction between *E. coli* HB101 and QCM-D AMP-coated sensors. This material is available free of charge via the Internet at http://pubs.acs.org.

AUTHOR INFORMATION

Corresponding Author

*Tel.: 508.831.5380. Fax: 508.831.5853. E-mail: terric@wpi.edu.

Notes

The authors declare no competing financial interest.

ACKNOWLEDGMENTS

This work was supported in part by the National Science Foundation (No. EEC 0754996) and a Grant-In-Aid of Research from Sigma Xi, the Scientific Research Society. The

authors would like to thank Ralf Richter and Prashant Sharma for helpful discussions.

REFERENCES

(1) Scallan, E.; Hoekstra, R. M.; Angulo, F. J.; Tauxe, R. V.; Widdowson, M. A.; Roy, S. L.; Jones, J. L.; Griffin, P. M. *Emerging Infect. Dis.* **2011**, *17*, 7−15.

(2) Rangel, J. M.; Sparling, P. H.; Crowe, C.; Griffin, P. M.; Swerdlow, D. L. *Emerging Infect. Dis.* **2005**, *11*, 603−609.

(3) Swaminathan, B.; Gerner-Smidt, P. *Microbes Infect.* **2007**, *9*, 1236−1243.

(4) Mattila, T.; Manninen, M.; Kyläsiurola, A.-L. *J. Dairy Res.* **1990**, *57*, 33−39.

(5) Tiller, J. C. *Adv. Polym. Sci.* **2011**, *240*, 193−217.

(6) Kügler, R.; Bouloussa, O.; Rondelez, F. *Microbiology (Reading, U.K.)* **2005**, *151*, 1341−1348.

(7) Tiller, J. C.; Lee, S. B.; Lewis, K.; Klibanov, A. M. *Biotechnol. Bioeng.* **2002**, *79*, 465−471.

(8) Waschinski, C. J.; Herdes, V.; Schueler, F.; Tiller, J. C. *Macromol. Biosci.* **2005**, *5*, 149−156.

(9) Crismaru, M.; Asri, L.; Loontjens, T. J. A.; Krom, B. P.; de Vries, J.; van der Mei, H. C.; Busscher, H. J. *Antimicrob. Agents Chemother.* **2011**, *55*, 5010−5017.

(10) Roe, D.; Karandikar, B.; Bonn-Savage, N.; Gibbins, B.; Roullet, J. B. *J. Antimicrob. Chemother.* **2008**, *61*, 869−876.

(11) Tiller, J. C.; Liao, C. J.; Lewis, K.; Klibanov, A. M. *Proc. Natl. Acad. Sci., U.S.A.* **2001**, *98*, 5981−5985.

(12) Murata, H.; Koepsel, R. R.; Matyjaszewski, K.; Russell, A. J. *Biomaterials* **2007**, *28*, 4870−4879.

(13) Costa, F.; Carvalho, I. F.; Montelaro, R. C.; Gomes, P.; Martins, M. C. L. *Acta Biomater.* **2011**, *7*, 1431−1440.

(14) Hancock, R. E. W.; Scott, M. G. *Proc. Natl. Acad. Sci., U.S.A.* **2000**, *97*, 8856−8861.

(15) Epand, R. M.; Vogel, H. J. *Biochim. Biophys. Acta, Biomembr.* **1999**, *1462*, 11−28.

(16) Shai, Y. *Biochim. Biophys. Acta, Biomembr.* **1999**, *1462*, 55−70.

(17) Brogden, K. A.; Ackermann, M.; McCray, P. B.; Tack, B. F. *Int. J. Antimicrob. Agents* **2003**, *22*, 465−478.

(18) Rossetto, G.; Bergese, P.; Colombi, P.; Depero, L. E.; Giuliani, A.; Nicoletto, S. F.; Pirri, G. J. *Nanomed. Nanotechnol.* **2007**, *3*, 198−207.

(19) Lad, M. D.; Birembaut, F.; Clifton, L. A.; Frazier, R. A.; Webster, J. R. P.; Green, R. J. *Biophys. J.* **2007**, *92*, 3575−3586.

(20) Oren, Z.; Shai, Y. *Biopolymers* **1998**, *47*, 451−463.

(21) Papo, N.; Shai, Y. *Peptides* **2003**, *24*, 1693−1703.

(22) Wang, K. F.; Nagarajan, R.; Mello, C. M.; Camesano, T. A. *J. Phys. Chem. B* **2011**, *115*, 15228−15235.

(23) Yeaman, M. R.; Yount, N. Y. *Pharmacol. Rev.* **2003**, *55*, 27−55.

(24) Shai, Y. *Biopolymers* **2002**, *66*, 236−248.

(25) Onaizi, S. A.; Leong, S. S. J. *Biotechnol. Adv.* **2011**, *29*, 67−74.

(26) Mason, A. J.; Bertani, P.; Moulay, G.; Marquette, A.; Perrone, B.; Drake, A. F.; Kichler, A.; Bechinger, B. *Biochemistry* **2007**, *46*, 15175−15187.

(27) Willcox, M. D. P.; Hume, E. B. H.; Aliwarga, Y.; Kumar, N.; Cole, N. *J. Appl. Microbiol.* **2008**, *105*, 1817−1825.

(28) Haynie, S. L.; Crum, G. A.; Doele, B. A. *Antimicrob. Agents Chemother.* **1995**, *39*, 301−307.

(29) Glinel, K.; Jonas, A. M.; Jouenne, T.; Leprince, J.; Galas, L.; Huck, W. T. S. *Bioconjugate Chem.* **2009**, *20*, 71−77.

(30) Gao, G. Z.; Lange, D.; Hilpert, K.; Kindrachuk, J.; Zou, Y. Q.; Cheng, J. T. J.; Kazemzadeh-Narbat, M.; Yu, K.; Wang, R. Z.; Straus, S. K.; Brooks, D. E.; Chew, B. H.; Hancock, R. E. W.; Kizhakkedathu, J. N. *Biomaterials* **2011**, *32*, 3899−3909.

(31) Bagheri, M.; Beyermann, M.; Dathe, M. *Antimicrob. Agents Chemother.* **2009**, *53*, 1132−1141.

(32) Cho, W. M.; Joshi, B. P.; Cho, H.; Lee, K. H. *Bioorg. Med. Chem. Lett.* **2007**, *17*, 5772−5776.

(33) Appendini, P.; Hotchkiss, J. H. *J. Appl. Polym. Sci.* **2001**, *81*, 609−616.

(34) Chen, R. X.; Cole, N.; Willcox, M. D. P.; Park, J.; Rasul, R.; Carter, E.; Kumar, N. *Biofouling* **2009**, *25*, 517−524.

(35) Gabriel, M.; Nazmi, K.; Veerman, E. C.; Amerongen, A. V. N.; Zentner, A. *Bioconjugate Chem.* **2006**, *17*, 548−550.

(36) Steven, M. D.; Hotchkiss, J. H. *J. Appl. Polym. Sci.* **2008**, *110*, 2665−2670.

(37) Oh, S. J.; Hong, B. J.; Choi, K. Y.; Park, J. W. *OMICS* **2006**, *10*, 327−343.

(38) Wong, L. S.; Khan, F.; Micklefield, J. *Chem. Rev. (Washington, DC, U.S.)* **2009**, *109*, 4025−4053.

(39) Rostovtsev, V. V.; Green, L. G.; Fokin, V. V.; Sharpless, K. B. *Angew. Chem., Int. Ed.* **2002**, *41*, 2596−2599.

(40) Lante, A.; Crapisi, A.; Pasini, G.; Scalabrini, P. *Biotechnol. Lett.* **1994**, *16*, 293−298.

(41) Hilpert, K.; Elliott, M.; Jenssen, H.; Kindrachuk, J.; Fjell, C. D.; Korner, J.; Winkler, D. F. H.; Weaver, L. L.; Henklein, P.; Ulrich, A. S.; Chiang, S. H. Y.; Farmer, S. W.; Pante, N.; Volkmer, R.; Hancock, R. E. W. *Chem. Biol.* **2009**, *16*, 58−69.

(42) Hemmersam, A. G.; Foss, M.; Chevallier, J.; Besenbacher, F. *Colloids Surf., B* **2005**, *43*, 208−215.

(43) Richter, R.; Mukhopadhyay, A.; Brisson, A. *Biophys. J.* **2003**, *85*, 3035−3047.

(44) Wickman, B.; Gronbeck, H.; Hanarp, P.; Kasemo, B. *J. Electrochem. Soc.* **2010**, *157*, B592−B598.

(45) Rodahl, M.; Hook, F.; Krozer, A.; Brzezinski, P.; Kasemo, B. *Rev. Sci. Instrum.* **1995**, *66*, 3924−3930.

(46) Iijima, N.; Tanimoto, N.; Emoto, Y.; Morita, Y.; Uematsu, K.; Murakami, T.; Nakai, T. *Eur. J. Biochem.* **2003**, *270*, 675−686.

(47) Sauerbrey, G. *Z. Phys. A: Hadrons Nucl.* **1959**, *155*, 206−222.

(48) Voinova, M. V.; Rodahl, M.; Jonson, M.; Kasemo, B. *Phys. Scr.* **1999**, *59*, 391−396.

(49) Reviakine, I.; Johannsmann, D.; Richter, R. P. *Anal. Chem.* **2011**, *83*, 8838−8848.

(50) Tsortos, A.; Papadakis, G.; Gizeli, E. *Biosens. Bioelectron.* **2008**, *24*, 836−841.

(51) Papadakis, G.; Tsortos, A.; Bender, F.; Ferapontova, E. E.; Gizeli, E. *Anal. Chem.* **2012**, *84*, 1854−1861.

(52) Dubois, L. H.; Nuzzo, R. G. *Annu. Rev. Phys. Chem.* **1992**, *43*, 437−463.

(53) Höök, F.; Vörös, J.; Rodahl, M.; Kurrat, R.; Böni, P.; Ramsden, J. J.; Textor, M.; Spencer, N. D.; Tengvall, P.; Gold, J.; Kasemo, B. *Colloids Surf., B* **2002**, *24*, 155−170.

(54) Tsortos, A.; Papadakis, G.; Mitsakakis, K.; Melzak, K. A.; Gizeli, E. *Biophys. J.* **2008**, *94*, 2706−2715.

(55) Gao, G.; Cheng, J. T. J.; Kindrachuk, J.; Hancock, R. E. W.; Straus, S. K.; Kizhakkedathu, J. N. *Chem. Biol.* **2012**, *19*, 199−209.

(56) Bagheri, M.; Beyermann, M.; Dathe, M. *Bioconjugate Chem.* **2012**, *23*, 66−74.

(57) Mechler, A.; Praporski, S.; Atmuir, K.; Boland, M. S., F.; Martin, L. L. *Biophys. J.* **2007**, *93*, 3907−3916.